Interfacial electronic structure at a metal–phthalocyanine/graphene interface: Copper–phthalocyanine versus iron–phthalocyanine*

Ye Wei-Guo(叶伟国), Liu Dan(刘 丹), Peng Xiao-Feng(彭啸峰), and Dou Wei-Dong(窦卫东)†

Physics Department, Shaoxing University, Shaoxing 312000, *China*

(Received 20 June 2013; revised manuscript received 16 July 2013)

The energy level alignment of CuPc and FePc on single-layer graphene/Ni(111) (SLG/Ni) substrate was investigated by using ultraviolet and X-ray photoelectron spectroscopy (UPS and XPS). The highest occupied molecular orbitals (HOMOs) in a thick layer of CuPc and FePc lie at 1.04 eV and 0.90 eV, respectively, below the Fermi level of the SLG/Ni substrate. Weak adsorbate–substrate interaction leads to negligible interfacial dipole at the CuPc/SLG/Ni interface, while a large interfacial dipole (0.20 eV) was observed in the case of FePc/SLG/Ni interface, due to strong adsorbate–substrate coupling. In addition, a new interfacial electronic feature was observed for the first time in the case of FePc on SLG/Ni substrate. This interfacial state can be attributed to a charge transfer from the SLG/Ni substrate to unoccupied orbitals of FePc.

Keywords: interfacial electronic structure, metal–phthalocyanine interface, graphene, workfunction

PACS: 73.20.–r, 73.30.+y, 73.22.Pr **DOI:** 10.1088/1674-1056/22/11/117301

1. Introduction

Interfacial electronic structures between organic semiconductors and conductive materials play central roles in organic devices,[1,2] such as organic light-emitting diodes (OLED) and organic photovoltaic (OPV) cells. Therefore, much work has been done on these structures.[3–9] The conductive electrodes serve as a source of charge in organic devices. The energy separation between the frontier orbitals of organic materials and the Fermi level of conductive electrodes determines the transfer barrier of either holes or electrons and therefore has substantial influence on the performance of the corresponding devices. Understanding the interfacial behavior of organic materials and conductive electrodes is vital in improving the performance of organic-based devices.

Graphene is a single layer of carbon atoms tightly packed into a two-dimensional (2D) honeycomb lattice.[10,11] Graphene materials have been broadly used as transparent anodes in devices such as OLED and OPV owing to graphene's brilliant mechanical flexibility, electric conductivity, and pellucidity.[12–16] Device performance can be substantially improved by using graphene as electrodes. Although a vast amount of work has been done to improve devices' performance, few studies focussed on the interfacial electronic structures between organic materials and graphene. However, knowledge about the organic/graphene interface is important because it is helpful for predicting the role of graphene in organic devices and therefore to provide guidance for choosing materials with matched energy levels. Moreover, in the case of metal–phthalocyanines (MPcs), adsorbate–substrate (AS) interaction can dramatically influence the magnetic properties of molecules, e.g., the molecular spin at a metal substrate surface can be partially quenched.[17,18] Recent work of Uihlein *et al.* found that a single layer of graphene can decouple cobalt–phthalocyanine (CoPc) from underlying Ni(111) substrate.[19] Therefore, the magnetic properties of CoPc are expected to be preserved. However, whether the decoupling can happen to other magnetic molecules such as FePc is still unknown. This was part of the motivation for our present work. In addition, MPcs usually show a good p-type transport nature and are frequently used as active layers in organic devices. Hence, MPc/graphene interfacial properties are important issues in the design of organic devices and therefore have attracted much attention.[20–23] A recent study demonstrated that the MPc/graphene interface can be influenced by the underlying layer of graphene.[24] This work is intended to cultivate a better understanding of this interface.

It is well known that interfacial electronic structures between organic materials and substrates are greatly influenced by the AS coupling strength. Strong AS coupling may induce charge exchange between MPc molecules and substrate, leading to the variation in energy position of frontier molecular orbitals with respect to the Fermi level of the substrate. As a result, the charge transfer barrier of a particular material differs from one substrate to another. The AS interaction between MPcs and graphene was recently studied by Yang *et al.* and Xiao *et al.* using scanning tunneling microscopy (STM),[25,26] by Scardamaglia *et al.* using photo-

*Project supported by the National Natural Science Foundation of China (Grant No. 61106131), the Natural Science Foundation of Zhejiang Province, China (Grant No. Y6110072), the Talents Project of Science and Technology Department of Qianjiang City, China (Grant No. 2012R10075), and the Postdoctoral Science Foundation of China (Grant No. 2012M521119).

†Corresponding author. E-mail: phyth@usx.edu.cn

© 2013 Chinese Physical Society and IOP Publishing Ltd

electron spectroscopy (PES),[18] and by Dou *et al.* using high-resolution electron energy-loss (HREEL) spectroscopy.[27] These studies demonstrated that MPc molecules prefer to lie flat on the graphene substrate. The flat-lying geometry favors AS coupling. More interestingly, graphene interacts more strongly with iron–phthalocyanine (FePc) than with copper–phthalocyanine (CuPc).[25,27] This is attributed to difference between the d-band populations in Fe and Cu. Therefore, it will be interesting to know the interfacial electronic structures of MPc/graphene when driven by different AS interactions.

In previous studies, we detailed the morphology and nucleating behavior of CuPc and FePc on graphene substrate.[28,29] Those findings are of particular interest with regard to various organic devices that can be based on graphene electrodes. In addition to the quality of organic film, the interfacial electronic structure between phthalocyanine and graphene is equally important for improving the performance of the corresponding devices. So far, little is known about this. Therefore, in the present study, we focus only on the interfacial electronic structure of two MPc specimens, CuPc and FePc, respectively, on SLG/Ni substrate. A previous PES study demonstrated a slight charge exchange between FePc and a graphene/Ir(111) substrate,[21] whereas no sign of interfacial electronic states was observed. In the present study, an interfacial state is observed in the case of FePc on SLG/Ni substrate. The interfacial electronic structures of CuPc and FePc on graphene substrate are found to be quite different, owing to the difference in adsorbate–graphene coupling.

2. Experimental

Graphene films were prepared on Ni(111) substrate surface in an ultra-high vacuum (UHV) chamber by cracking propylene (C_3H_6). The Ni(111) substrate was first heated up to 700 °C in UHV, then cooled down to 500 °C within 5 min in the presence of C_3H_6 at a pressure of 1×10^{-6} mbar. The high quality of the resulting graphene sample was confirmed by using atomic force microscopy (AFM) and Raman measurement in ambient conditions (see Fig. 1). The organic depositions and PES measurements were performed in another UHV system. The graphene/Ni(111) substrate was annealed at 150 °C for half an hour in the UHV chamber to remove air contaminations. The substrate was cooled to room temperature before PES measurements and organic deposition. CuPc and FePc films were deposited on graphene samples step by step via thermal evaporation with a deposition rate of 0.5 Å/min. The thickness (Θ) of the organic layers was monitored with a quartz microbalance. Our previous study revealed that the first adlayer is completed at film thickness of 3.2 Å.[27] Here, we assume the thickness of a multilayer to be a simple multiple of the thickness of the first layer. All of the PES measurements were performed in a VG ESCALAB 220i-XL UHV surface analysis system. HeI ($h\nu = 21.22$ eV) light was used for the UPS experiments.

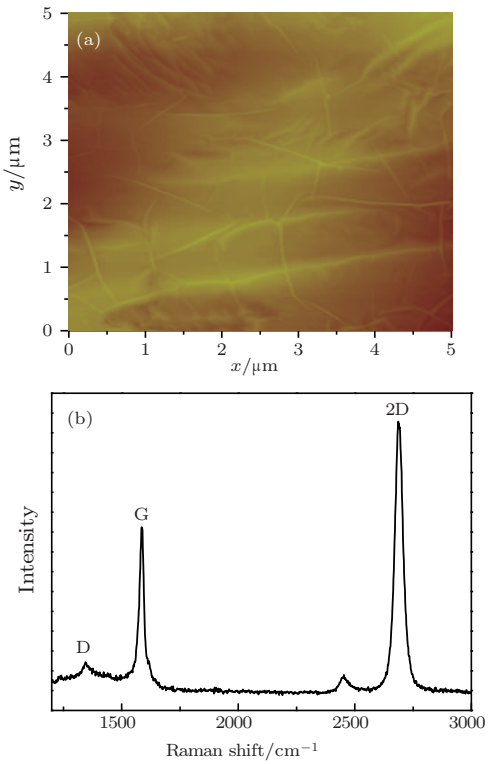


Fig. 1. (color online) (a) AFM and (b) Raman spectra of single-layer graphene on Ni(111) substrate.

3. Results and discussion

Figure 2 shows the UPS results and the corresponding workfunction of CuPc film on SLG/Ni substrate at various film thicknesses. The uppermost spectrogram in Fig. 2(a) shows the typical valence electronic feature of SLG (Gr. 2π) and the underlying Ni substrate (Ni 3d). The signal of Ni valence states slowly decreases with the increase in the CuPc film thickness. However, this signal does not vanish at multilayer coverage, e.g., it is still visible even at the film thickness of $\Theta = 20$ Å as indicated by the non-zero signal at the vicinity of Fermi level. Considering the surface-sensitive nature of UPS measurements, this indicates that the surface of the graphene substrate is not fully covered by CuPc at this coverage stage. This conclusion is consistent with our previous atomic force microscope (AFM) observation of CuPc film grown on graphene/Ni(111) substrate.[28] The 2π valence electronic feature of SLG is less detectable upon the deposition of CuPc film because this feature is energetically mixed with the π-relative orbital of the CuPc molecule. The peak intensity of CuPc HOMO gradually becomes stronger with the growth of the CuPc film, while the energy position of this peak does not shift significantly during the step-by-step deposition process. A similar phenomenon is also observed for the π-related features of CuPc. This indicates a quite weak adsorbate–substrate coupling between CuPc and SLG

substrate. This observation is in good agreement with our previous HREEL study,[27] and the UPS work of Wu *et al.* on similar graphene substrate.[24] Figures 2(b) and 2(c) show respectively the variation in secondary electron cutoff (SEC) of UPS data at various CuPc film thicknesses and the corresponding workfunctions deduced from the equation below,

$$\Phi = h\nu - \mathrm{BE_{SEC}}, \tag{1}$$

where Φ is the workfunction organic/SLG/Ni sample at various film thickness Θ; $\mathrm{BE_{SEC}}$ represents the corresponding binding energy of SEC in the UPS data. Figure 2(c) shows a slight increase in workfunction upon the adsorption of CuPc on SLG/Ni substrate. The workfunction increases slightly as the CuPc film thickness increases from 0 to 20 Å. The total shifted value is ~ 0.03 eV.

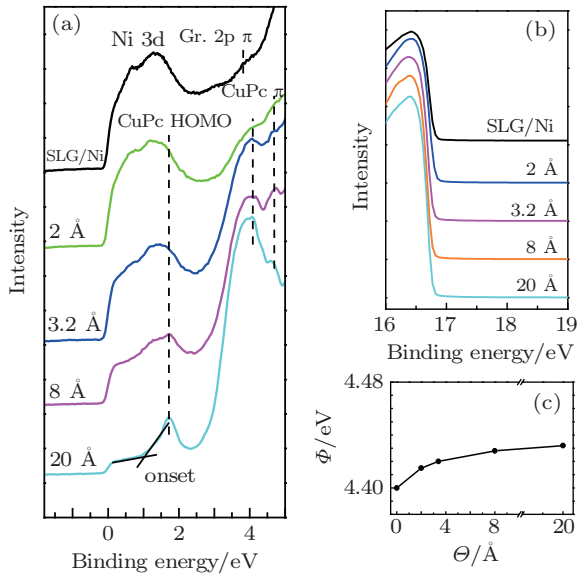


Fig. 2. (color online) (a) Valence states, (b) secondary electron cutoff, and (c) workfunction of CuPc on SLG/Ni substrate for various film thicknesses.

Previous studies showed that graphene substrate is more strongly coupled with FePc than with CuPc.[22,24] It is interesting to discover the interfacial electronic structure of FePc/graphene, since the stronger AS interaction usually leads to new electronic structures that are not comparable with those of CuPc. Figures 3(a) and 3(b) show the valence features of FePc on graphene at various film thicknesses. Figure 3(c) shows the variation of SEC, from which the corresponding workfunctions (see Fig. 3(d)) were deduced according to Eq. (1). The workfunction substantially rises from 4.40 eV for bare graphene/Ni to 4.55 eV for 1-Å FePc on graphene/Ni substrate (see Fig. 3(d)), and then reaches 4.71 eV when the film thickness increases further to 3.2 Å. Over this coverage stage, the workfunction shows no variations. Therefore, the maximum change of workfunction is calculated to be 0.31 eV for FePc films on graphene, which is remarkably larger than that of CuPc.

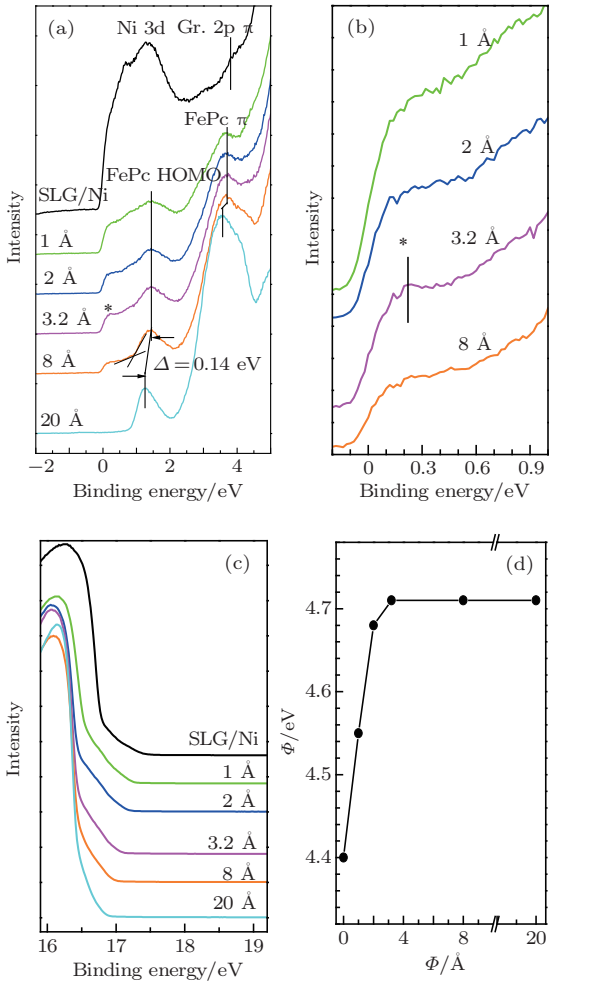


Fig. 3. (color online) (a) and (b) Valence states, (c) secondary electron cutoff, and (d) workfunction of FePc on SLG/Ni substrate for various film thicknesses.

Upon closely surveying the changes of valence states in the UPS spectra of FePc on graphene, other distinctive factors of CuPc were observed. First of all, the peak position of FePc HOMO of the first organic layer (interfacial phase) is shifted to some extent ($\Delta = 0.11$ eV) toward higher binding energy compared to that of the thin-film phase (see Fig. 3(a)). A similar energy shift is observed for some π-related molecular orbitals (marked with FePc π in Fig. 3(a)) with higher binding energy than the HOMO, while in the case of CuPc, a similar shift in the energy position of the HOMO was not observed. The shift in the energy position of FePc's orbital indicates a strong AS interaction between FePc and graphene. Upon close scrutiny of the UPS data of FePc on graphene, one can also observe a new feature (marked with an asterisk) peaked at the vicinity of Fermi level. This feature is superimposed with the PE emission of the Ni 3d electronic band, and is therefore less predominant than the Ni 3d signal. To distinguish this new feature, we show in Fig. 3(b) the details of the variation of PE emission with binding energy of 0–1 eV. This feature is slightly detectable at a film thickness of 2 Å and then becomes clearly visible at the film thickness of 3.2 Å. It is worth noting that this feature vanishes at multilayer cover-

age, e.g., $\Theta > 3.2$ Å. According to our previous studies,[27] the first FePc adlayer is saturated at film thickness of 3.2 Å. Therefore, the disappearance of the asterisk feature in the UPS of FePc over the first adlayer on graphene indicates that the asterisk feature is an interfacial state (IS), which is most probably induced by the strong AS coupling between FePc and the graphene/Ni substrate. In our previous HREELS study, we observed that FePc interacts with graphene substrate through an Fe-related orbital.[27] This finding has been further supported by the recent work of Scardamaglia *et al.* who demonstrated that the electronic structure of the FePc macrocycles is preserved while the Fe-based orbitals experience a slight modification upon adsorption on a graphene/Ir(111) substrate.[21] In addition, the recent DFT work of Sandin implies a considerable electronic intermixing between FePc and the graphene-π band, which is mediated by the lowest unoccupied molecular orbital (LUMO) of FePc and localized to the central Fe atom of the molecule.[30] This implies an electron transfer from graphene to the Fe-related LUMO state of FePc upon adsorption. The same conclusion can be drawn from observation of the Fano-line shaped Raman-active vibration mode in HREEL spectra of single-layer FePc on graphene/Ni(111) substrate since this asymmetric HREEL spectroscopic feature appears only if the LUMO of the adsorbate overlaps the Fermi level of the substrate to a considerable extent.[27,31–36] Based on this knowledge, it can be concluded that the asterisk state originates from the filling of the unoccupied Fe-related states.

The d band intensity of Ni substrate declines dramatically upon the deposition of FePc even at early deposition stage, e.g., $\Theta = 1$ Å and then this peak becomes completely undetectable when FePc film thickness reaches 20 Å. This phenomenon is in discrepancy with the case of CuPc. Recall that this signal is still clearly detectable at the film thickness stage of 20 Å in the case of CuPc. This discrepancy gives rise to a film morphology for FePc that differs from that of CuPc. In the case of FePc, the surface of the graphene/Ni substrate is completely covered by organic adlayers at a film thickness of 20 Å, while in the case of CuPc, at this coverage stage, a large portion of the graphene surface is still not covered by organic film.[29] Thus, Ni 3d emission is completely quenched at the multilayer coverage stage of FePc on SLG/Ni(111) substrate, while in the case of CuPc, this signal is still detectable at the same film thickness.

The UPS results show doubtlessly a much stronger AS interaction for FePc/graphene than for CuPc/graphene. To further support this claim, we compare the XPS results of CuPc and FePc on graphene substrate as shown in Figs. 4 and 5, respectively. For CuPc (see Fig. 4), all of the photoemission features of CuPc remain unchanged during the increase in the film thickness. This indicates undetectable electron transfer between CuPc and the graphene substrate, which is consistent with our UPS observations. We note a slight blue-shift of the C_{1s} feature of the graphene sample compared to that of the CuPc film. The C_{1s} feature of bare graphene, i.e., $\Theta = 0$ Å, is a single peak (284.92 eV) and represents the C–C bond of graphene. While three peaks are resolved for the C_{1s} peak of CuPc, representing respectively the C–C bond of the benzene ring (284.77 eV), the C–N bond of the CN macrocycle (286.22 eV), and a satellite peak (288.09 eV). The blue shift of the C–C feature of graphene compared with that of CuPc results from strong graphene–Ni substrate coupling, as has been well established in the Ref. [37]. For FePc (see Fig. 5), the C_{1s} and Ni_{2p} features are similar to those of CuPc, while N_{1s} and Fe_{2p} features obviously change in different ways from those of CuPc. N_{1s} is located at a lower binding energy position at the interfacial film stage, e.g., $\Theta = 3.2$ Å, than at the thick film stage, e.g., $\Theta = 20$ Å. Fe_{2p} features also have such a red-shift phenomenon but with a larger shift of 0.20 eV (see f2 for example). This indicates that FePc obtains electrons when it adsorbs on graphene and the transferred electrons are mainly located on the N–Fe group of FePc. This finding is consistent with our previous HREELS observation.[27] In addition, a new feature can be observed at $E_b = 709.05$ eV. We interpret it as a hybrid state of the Fe atom of FePc with the graphene substrate.

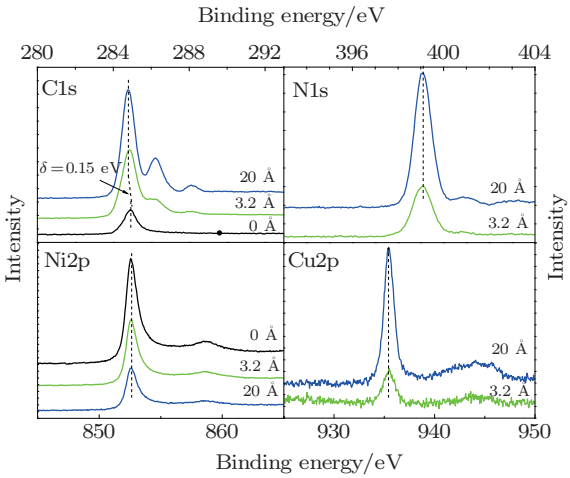


Fig. 4. (color online) XPS of CuPc on graphene/Ni substrate with various film thicknesses.

Our previous HREELS study revealed that FePc interacts with graphene through an Fe-related molecular orbit.[27] Sandin's theoretical work confirmed our observation, and he further observed a gap state which has been established as a delocalized hybrid graphene–adsorbate state with density on both graphene substrate and the Fe atom of FePc.[30] Therefore, electron redistribution can be expected to occur at the FePc/graphene interface. All of these phenomena are instances of strong FePc–graphene interaction. These observations agree well with the UPS findings.

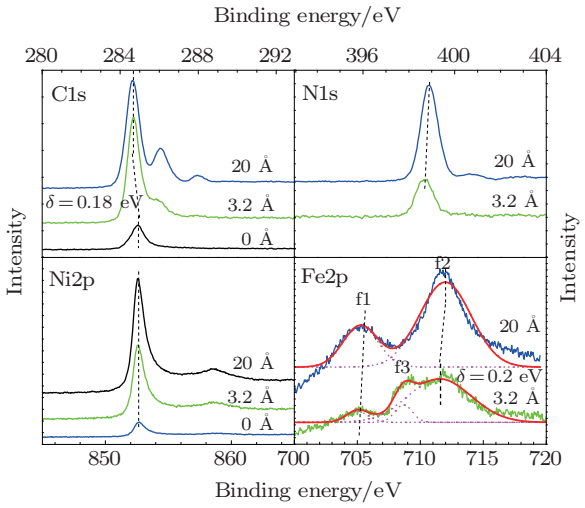


Fig. 5. (color online) XPS of FePc on graphene/Ni substrate for various film thicknesses. The Fe_{2p} feature at interfacial and thick film stage is fitted with three and two Gaussian lines respectively in order to evaluate the energy shift value and to distinguish the new peak.

The interfacial energy level diagrams of CuPc and FePc films on SLG/Ni substrate are shown in Fig. 6. The workfunction of SLG/Ni substrate is measured as 4.40 eV. The alignment of the energy levels of CuPc and FePc relative to the Fermi level were deduced from the measured HOMO at the onset of the corresponding peaks, assuming an unaltered band gap of 2.3 eV for CuPc and 2.6 eV for FePc.[38,39] The position of the vacuum level (VL) is determined by considering the workfunction at various film thicknesses. The hole and electron injection barriers (Φ_h and Φ_e) of CuPc on SLG/Ni substrate are calculated to be 1.04 eV and 1.26 eV, respectively. The Φ_e is slightly larger than Φ_h, which indicates a p-type transport nature for CuPc on a graphene-covered Ni electrode. This is consistent with the recent UPS report of CuPc on graphene.[21] The Φ_h value of CuPc/graphene interface is close to that of the CuPc/Au interface (0.90 eV),[40] making it a good alternative to gold as an electrode material. The height of the hole injection barrier, Φ_h of FePc on graphene/Ni can be deduced by considering the onset of the HOMO of FePc thin film ($\Theta = 2$ Å) at a binding energy of 0.79 eV and the band bending of the HOMO (0.11 eV). The Φ_h of FePc is calculated to be 0.90 eV, which is much smaller than the electron injection barrier, $\Phi_e = 1.70$ eV. Therefore, FePc also shows p-type transport nature on graphene/Ni substrate, similar to the case of CuPc. In addition, the existence of the FePc/graphene interface may further reduce the hole injection barrier, facilitating the charge transfer between the organic layer and the graphene electrode.[41] The dipole (eD) across the interface between MPc and graphene/Ni can be calculated by subtracting the value of the band bending of vacuum level ($VL_B = 0$ for CuPc and 0.11 eV for FePc) from the maximum shifted value of the workfunction. The dipole value is calculated to be 0.03 eV for CuPc and 0.20 eV for FePc. The small dipoles are another advantage when designing organic devices based on electrodes of MPc on SLG/Ni.

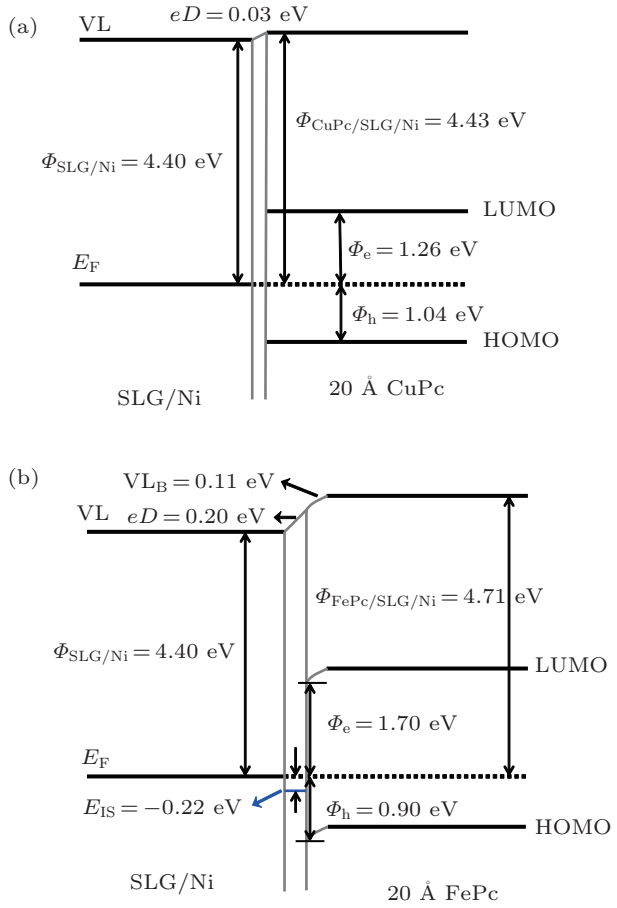


Fig. 6. Interfacial energy level diagram of CuPc (a) and FePc (b) on SLG/Ni substrate.

4. Conclusion

In summary, the valence electronic characters of CuPc/SLG/Ni and FePc/SLG/Ni were discovered through PES measurements. The HOMO of CuPc lies 1.04 eV below the Fermi level of graphene/Ni substrate, giving a hole-injection barrier of 1.04 eV. The energy position of the FePc HOMO is slightly closer to the Fermi level than that of CuPc, leading to a smaller hole injection barrier of 0.90 eV. The energy position of CuPc HOMO is unchanged when the molecule adsorbs on graphene/Ni substrate, evidencing a very weak AS coupling in the case of CuPc on graphene/Ni substrate. In addition, this weak coupling leads to a negligible interfacial dipole (0.03 eV) which is an advantage for hole injection from a graphene/Ni electrode to the CuPc film. In contrast, the HOMO position of FePc in the first single layer is shifted toward higher binding energy than that of FePc molecules in multilayers, indicating a strong AS coupling in this case. An interfacial electronic feature was also observed for the first time in the UPS taken from the first layer of FePc on graphene/Ni, which has been attributed to a charge transfer from graphene/Ni to an Fe-related unoccupied orbital of FePc.

References

[1] Ishii H, Sugiyama K, Ito E and Seki K 1999 *Adv. Mater.* **11** 605
[2] Braga D and Horowitz G 2009 *Adv. Mater.* **21** 1473
[3] Crispin X, Geskin V, Crispin A, Cornil J, Lazzaroni R, Salaneck W R and Brédas J L 2002 *J. Am. Chem. Soc.* **124** 8131
[4] Koch N, Heimel G, Wu J, Zojer E, Johnson R L, Brédas J L, Müllen K and Rabe J P 2005 *Chem. Phys. Lett.* **413** 390
[5] Koch N, Duhm S, Rabe J P, Vollmer A and Johnson R L 2005 *Phys. Rev. Lett.* **95** 237601
[6] Petraki F and Kennou S 2009 *Org. Electron.* **10** 1382
[7] Wang N N, Yu J S, Zang Y and Jiang Y D 2010 *Chin. Phys. B* **19** 038602
[8] Cao G H, Qin D S, Guan M, Cao J S, Zeng Y P and Li J M 2007 *Chin. Phys. Lett.* **24** 1380
[9] Müller K, Seitsonen A P, Brugger T, Westover J, Greber T, Jung T and Kara A 2012 *J. Phys. Chem. C* **116** 23465
[10] Geim A K and Novoselov K S 2007 *Nat. Mater.* **6** 183
[11] Pan Y, Shi D X and Gao H J 2007 *Chin. Phys.* **16** 3151
[12] Ma P, Jin Z, Guo J N, Pan H L, Liu X Y, Ye T C, Wang H and Wang G Z 2012 *Chin. Phys. Lett.* **29** 057302
[13] Wu J B, Agrawal M, Becerril H A, Bao Z N, Liu Z F, Chen Y S and Peumans P 2009 *ACS Nano* **4** 43
[14] Kang S, Kim J B, Kim K S, Zhao Y, Chen Z, Lee G H, Hone J, Kim P and Nuckolls C 2011 *Adv. Mater.* **23** 3531
[15] Liu Z F, Liu Q, Huang Y, Ma Y F, Yin S, Zhang X Y, Sun W and Chen Y S 2008 *Adv. Mater.* **20** 3924
[16] Wu J B, Becerril H A, Bao Z N, Liu Z F, Chen Y S and Peumans P 2008 *Appl. Phys. Lett.* **92** 263302
[17] Fu Y S, Ji S H, Ma X C, Wu R, Wang C C, Duan W H, Qiu X H, Sun B, Zhang P, Jia J F and Xue Q K 2007 *Phys. Rev. Lett.* **99** 256601
[18] Schmid M, Kaftan A, Steinruck H P and Gottfried J M 2012 *Surf. Sci.* **606** 945
[19] Uihlein J, Peisert H, Glaser M, Polek M, Adler H, Petraki F, Ovsyannikov R, Bauer M and Chassé T 2013 *J. Chem. Phys.* **138** 081101
[20] Mao H Y, Wang R, Wang Y, Niu T C, Zhong J Q, Huang M Y, Qi D C, Loh K P, Wee A T S and Chen W 2011 *Appl. Phys. Lett.* **99** 093301
[21] Scardamaglia M, Lisi S, Lizzit S, Baraldi A, Larciprete R, Mariani C and Betti M G 2013 *J. Phys. Chem. C* **117** 3019
[22] Ren J, Meng S, Wang Y L, Ma X C, Xue Q K and Kaxiras E 2011 *J. Chem. Phys.* **134** 194706
[23] Xu H, Xie L, Zhang H and Zhang J 2011 *ACS Nano* **5** 5338
[24] Wu Q H, Hong G, Ng T W and Lee S T 2012 *Appl. Phys. Lett.* **100** 161603
[25] Yang K, Xiao W D, Jiang Y H, Zhang H G, Liu L W, Mao J H, Zhou H T, Du S X and Gao H J 2012 *J. Phys. Chem. C* **116** 14052
[26] Xiao K, Deng W, Keum J K, Yoon M, Vlassiouk I V, Clark K W, Li A P, Kravchenko I I, Gu G, Payzant E A, Sumpter B G, Smith S C, Browning J F and Geohegan D B 2013 *J. Am. Chem. Soc.* **135** 3680
[27] Dou W D, Huang S P, Zhang R Q and Lee C S 2011 *J. Chem. Phys.* **134** 094705
[28] Dou W D, Yang Q D and Lee C S 2012 *J. Phys. Chem. C* **116** 19278
[29] Dou W D, Yang Q D and Lee C S 2013 *Appl. Phys. Lett.* **102** 131606
[30] Sandin A A T 2012 *Tunneling Spectroscopy Studies of Epitaxial Graphene on and Its Interfaces* (Ph.D dissertation)
[31] Amsalem P, Giovanelli L, Themlin J M and Angot T 2009 *Phys. Rev. B* **79** 235426
[32] Tautz F S, Eremtchenko M, Schaefer J A, Sokolowski M, Shklover V and Umbach E 2002 *Phys. Rev. B* **65** 125405
[33] Kröger J 2006 *Rep. Prog. Phys.* **69** 899
[34] Chabal Y J 1985 *Phys. Rev. Lett.* **55** 845
[35] Hirschmugl C J, Williams G P, Hoffman F M and Chabal Y J 1990 *Phys. Rev. Lett.* **65** 480
[36] Kröger J, Lehwald S and Ibach H 1997 *Phys. Rev. B* **55** 10895
[37] Giovannetti G, Khomyakov P A, Brocks G, Karpan V M, van den Brink J and Kelly P J 2008 *Phys. Rev. Lett.* **101** 026803
[38] Hill I G, Kahn A, Soos Z G and Pascal R A 2000 *Chem. Phys. Lett.* **327** 181
[39] Sharma G D, Krumar R and Roy M S 2006 *Sol. Energy Mater. Sol. Cells* **90** 32
[40] Chen W, Huang C, Gao X Y, Wang L, Zhen C G, Qi D C, Chen S, Zhang H L, Loh K P, Chen Z K and Wee A T S 2006 *J. Phys. Chem. B* **110** 26075
[41] Zhong S, Zhong J Q, Mao H Y, Zhang J L, Lin J D and Chen W 2012 *Phys. Chem. Chem. Phys.* **14** 14127